RSC Advances

PAPER

View Article Online
View Journal | View Issue

Cite this: *RSC Adv.*, 2020, **10**, 21082

Preparation of activated carbon from *Dipterocarpus alatus* fruit and its application for methylene blue adsorption†

Chantakorn Patawat,[a] Ketsara Silakate,[a] Somchai Chuan-Udom,[b] Nontipa Supanchaiyamat,[c] Andrew J. Hunt[c] and Yuvarat Ngernyen*[a]

Activated carbons were prepared from three parts of *Dipterocarpus alatus* fruit (wing, endocarp and pericarp), an abundant and renewable waste in Southeast Asia, by chemical activation using $ZnCl_2$, $FeCl_3$, H_3PO_4 and KOH and physical activation using CO_2 and steam. This study indicated that activated carbon prepared from *Dipterocarpus alatus* fruit could be employed as a promising adsorbent for the removal of methylene blue from aqueous solution. $ZnCl_2$ activation led to an activated carbon with a surface area of 843 m^2 g^{-1} and was able to remove methylene blue from aqueous solution. Adsorption studies were performed and analysed using Langmuir and Freundlich isotherm equations. Adsorption data demonstrated an excellent fit with the Langmuir isotherm model, with the maximum adsorption capacity of 269.3 mg g^{-1} at equilibrium. Pseudo-first order and pseudo-second order kinetic models were used in this study to describe the adsorption mechanism. The results show that methylene blue adsorption is pseudo-second order, indicating that liquid film diffusion, intra-particle diffusion and surface adsorption coexisted during methylene blue adsorption on the activated carbon. The activated carbon prepared from *Dipterocarpus alatus* fruit is a low cost and effective adsorbent with a fast rate for the removal of methylene blue from aqueous solutions when compared with a number of activated carbons studied in the literature.

Received 17th April 2020
Accepted 28th May 2020

DOI: 10.1039/d0ra03427d

rsc.li/rsc-advances

1 Introduction

An increase in the world's population has led to greater demand for various industrial products. Dyes are extensively utilised by many industries such as textiles, leather tanning, paper production, printing, food technology, plastics, hair colourings, *etc.*[1] Up to 15% of the dye is lost in the effluent during the dyeing process, thus causing environmental problems.[2] Significant numbers of dyes are considered toxic to aquatic life and stable to light, making them difficult to degrade and persistent in the environment.[3] Methylene blue (MB) is a basic or cationic dye with commonly used in various applications such as colouring and dyeing cotton, wool and silk.[4] MB has various harmful effects on human beings, including increased heart rate, vomiting, shock, cyanosis, jaundice, quadriplegia and tissue necrosis.[5] Therefore, it is importance for dyes to be removed from wastewater to ensure local human populations and also the environment remain healthy.

Various treatment methods have been used for the removal of dyes from industrial wastewater, including membrane filtration, electrochemical degradation, bioremediation, biodegradation, coagulation/flocculation, chemical precipitation, chemical oxidation, ozonation and photocatalysis.[6–9] However, adsorption process is a well-established and powerful technique for treating industrial wastewater due to high efficiency, flexibility and simplicity of design, convenience of operation and low cost of appropriate adsorbent materials.[6,10]

Activated carbon have found use in a wide variety of applications including used as an adsorbent, electrodes for supercapacitor,[11,12] catalysts,[13] additives,[14] synthesis of 5-hydroxymethylfurfural,[15] or for bitumen modification[16] to name but a few. In addition, activated carbon is amongst the most used adsorbent utilised due to its high surface area, pore volumes, fast adsorption rate and high adsorption capacity. In general, preparation of activated carbon is carried out by physical or chemical activation. Physical activation method consists of two steps; carbonisation of raw material and then activation with CO_2, steam or air. Chemical activation is a single step that activation of raw material with a chemical activating agent such as $ZnCl_2$, $FeCl_3$, H_3PO_4, H_2SO_4, NaOH or KOH.

[a]*Biomass & Bioenergy Research Laboratory, Department of Chemical Engineering, Faculty of Engineering, Khon Kaen University, Khon Kaen, 40002, Thailand. E-mail: nyuvarat@kku.ac.th*

[b]*Department of Agricultural Engineering, Faculty of Engineering, Khon Kaen University, Khon Kaen, 40002, Thailand*

[c]*Materials Chemistry Research Center, Department of Chemistry and Center of Excellence for Innovation in Chemistry, Faculty of Science, Khon Kaen University, Khon Kaen, 40002, Thailand*

† Electronic supplementary information (ESI) available. See DOI: 10.1039/d0ra03427d

Frequently commercial activated carbons are coal derived and are of higher cost, as such agricultural by-products and waste materials have been used as raw materials in producing activated carbons.[7,17]

Dipterocarpus alatus is a tropical forest tree that can grow in many countries of Southeast Asia such as Thailand, Laos, Myanmar, Vietnam and Philippines. Fruit is a winged nut of 1.5–2 cm in diameter. The wings develop from the persistent sepals that are 11–14 cm long and 1.5–2 cm wide. The colour of fruit is pink red when young, yellowish when mature and when ripe, the colour change to brown and falls from the tree. The nut compose of seed enclosed with endocarp and has pericarp at outer. Many parts of this tree had benefits such as oil is used as biodiesel, wood used in construction or bark can used as herb.[18] However, the falling fruits are lignocellulosic wastes with no current method of utilisation. Importantly, to date no studies have been reported on the preparation of activated carbon from *Dipterocarpus alatus* fruit (DF). The use of this waste as feedstock not only leads to a range of new activated carbon materials but may also be adventurous in terms of availability and cost.

Herein, activated carbons from DF have been prepared by chemical activation with $ZnCl_2$, $FeCl_3$, H_3PO_4 and KOH and physical activation with CO_2 and steam. The porous properties, chemical functionality surface morphology of the prepared activated carbons were performed by N_2 adsorption, FTIR, SEM, and pH_{pzc}. Activated carbons of DF were tested in the removal of methylene blue dye from aqueous solutions. The influence of contact time and initial concentration on the adsorption is investigated, in addition to adsorption isotherms of MB on the prepared activated carbons. The kinetic and equilibrium data of the adsorption were analysed to study mechanisms of adsorption.

2 Materials and methods

2.1 Preparation of the precursor material

The *Dipterocarpus alatus* fruits (DF) used in this study were collected on the Khon Kaen University, Thailand. Fruits were separated into wing, endocarp and pericarp and then cutting into small pieces (see Fig. 1). The various parts of the DF were sieved with a 4 mm (mesh no. 5).

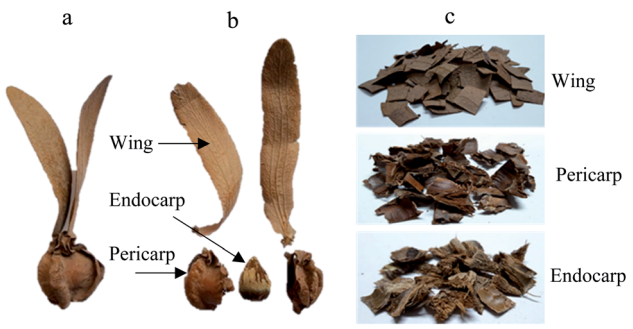

Fig. 1 Photographs of (a) ripe DF; each part of DF: (b) before cutting; (c) after cutting.

The thermal behaviour of DF was measured with a thermogravimetric analyser (Shimadzu, TGA-50). 10 mg of sample was heated from 25 to 700 °C at a ramping rate of 10 °C min^{-1} under N_2 atmosphere with the flow rate of 200 mL min^{-1}.

2.2 Synthesis of activated carbons

Biomass (about 10 g) was immersed in an aqueous solution containing 30 wt% of $ZnCl_2$, $FeCl_3$, H_3PO_4 or KOH for 24 h with the impregnation ratio of biomass:chemical activator of 1 : 2 by weight, followed by carbonized at 500 °C in N_2 (200 mL min^{-1}) for 1 h. The resulting activated carbons were then washed with distilled water for several times to remove residual chemical until the pH of the filtrate reaches 7. The samples were then dried at 120 °C for 6 h in an oven to obtain the activated carbons that ready to use.

The physically activated carbons were synthesised with a two steps process: the precursor was carbonized at 400 °C in a N_2 stream (200 mL min^{-1}) for 1 h, the resulting biochar was then activated at 850 °C in CO_2 (200 mL min^{-1}) or steam (12 mL min^{-1}) for 1 h.

The activated carbon production yield was calculated as follows:

$$\text{Yield}(\%) = \frac{m_f}{m_i} \times 100 \quad (1)$$

where m_f is the weight of the produced activated carbon and m_i is the weight of the raw precursor.

2.3 Characterisation of activated carbon

The specific surface area and pore structure parameters of the prepared activated carbons were evaluated by N_2 adsorption–desorption isotherm using a surface area and porosity analyser (ASAP2460, Micromeritics) at 77 K. The BET surface area (S_{BET}) was calculated by the Brunauer–Emmett–Teller equation. The micropore volume (V_{mic}) was determined by *t*-plot method. The total pore volume (V_T) was determined from the amount of N_2 adsorbed at the relative pressure (P/P^o) around 0.99. The mesopore volume (V_{meso}) was calculated by subtracting V_{mic} from V_T. The average pore diameter (D_P) was calculated from the Barrett–Joyner–Halenda (BJH) method.

Surface morphology of activated carbon was observed by using a scanning electron microscopy (SEM, Leo 1450 VP). A working voltage of 17 kV and the magnification of ×1000 was utilised. Surface functional groups of the activated carbon sample were detected by Fourier Transform Infrared (FTIR) spectroscopy (TENSOR 27, Bruker) using a potassium bromide (KBr) pellet. The spectrum was recorded between 4000–600 cm^{-1}.

The pH at the point of zero charge (pH_{pzc}) was determined using the pH drift method. A series of 0.01 M NaCl solutions were prepared at different initial pH between 2 to 12. Dilute solutions of 0.1 M HCl and NaOH were used for adjustment of pH values. 0.15 g of activated carbon was added to 50 mL of NaCl solution and then the sample was shaken using an orbital shaker (GALLENKAMP) at 120 rpm for 48 h. The final pH values were measured with pH meter (OHAUS, STARTER3100) and

plotted against initial pH of the solution. pH_{pzc} is determined as the point where the curve pH_{final} *vs.* $pH_{initial}$ intersects the line $pH_{initial} = pH_{final}$.

2.4 Adsorption experiments

The prepared activated carbon with highest surface area was used in adsorption studies. For the adsorption kinetics experiments, the MB solution of 6.0 mg L^{-1} was used. MB solution of 50 mL was placed in 250 mL Erlenmeyer flask and approximately 10.0 mg of activated carbon was put into this solution. The sample was shaken with an orbital shaker (GALLENKAMP) at a constant speed of 120 rpm for the allotted contact time (10–300 min). Activated carbon and MB solutions were separated by centrifuging (Hettich ROTOFIX 32 A) at 3500 rpm for 10 min. Dye concentration in the solution was measured at 665 nm using UV-visible spectrophotometer (Analytik-Jena AG). Blank containing no dye was used as controls and a calibration curve of absorbance *versus* concentration was constructed.

Equilibrium adsorption studies were carried out by mixing 10.0 mg of activated carbon samples with 50 mL solutions of various MB concentrations ranging from 6.0 mg L^{-1} to 450.0 mg L^{-1} without adjusting pH (between pH 6.0–6.5). Flasks were shaken until equilibrium was reached. Dilutions were made when absorbance from UV-visible spectrophotometer exceeded 1.2.

Adsorption capacity at time t (q_t, mg g^{-1}) and equilibrium adsorption capacity (q_e, mg g^{-1}) were determined by eqn. (2) and (3), respectively:

$$q_t = \frac{(C_0 - C_t)V}{m} \quad (2)$$

$$q_e = \frac{(C_0 - C_e)V}{m} \quad (3)$$

where C_0 is the actual MB initial concentration (mg L^{-1}), C_t is the MB concentration at time t (mg L^{-1}), C_e is the MB equilibrium concentration (mg L^{-1}), m is the actual amount of adsorbent (g) and V is the volume of dye solution (50×10^{-3} L).

3 Results and discussion

3.1 Initial characterisation of DF

Table 1 presents the proximate analysis of the each part of DF. It can be observed that DF presents low ash and high volatile matter content, similar to other biomass residuals that have been reported in literature for the production of activated carbon.[19–22] The fixed carbon content of DF (16.0–17.3%) is also comparable with other biomass wastes feedstock for production of activated carbon materials such as walnut shell (15.9%),[23] almond tree pruning (16.0%),[23] sugarcane bagasse (16.4%),[24] barley straw (17.3%),[19] rice-straw (17.8%),[25] peach stone (17.9%),[26] and paulownia wood (18.9%).[22]

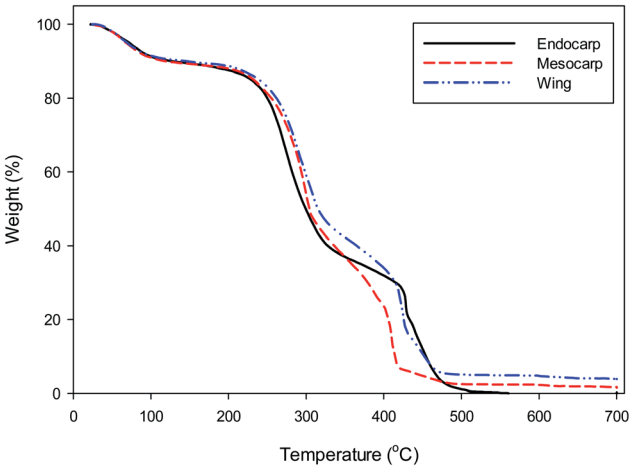

Fig. 2 TG curves for DF.

TGA analysis of the DF is presented in Fig. 2. The initial weight loss occurring between 25–200 °C could be attributed to water loss and some organic compounds. The main weight loss in the second stage from 200 to 500 °C may be associated with the thermal decomposition reaction of hemicellulose, cellulose and lignin.[28,29] The final weight loss at 500–700 °C was insignificant, implying that the decomposition reactions were almost completed. Therefore, the suitable temperature for preparation of activated carbon should be at least 500 °C.

3.2 Porous properties of activated carbons

The DF activated carbons (AC) were prepared by chemical activation with $ZnCl_2$, $FeCl_3$, H_3PO_4 and KOH and physical activation with CO_2 and steam. The chemically activated carbons were prepared by direct carbonised of the precursors impregnated with chemical agents. Nitrogen gas adsorption–desorption isotherms for the prepared activated carbon are shown in Fig. S1.† The types of the activating agent seem to have a significant influence on the shape of isotherms. The isotherms were of Type I and IV according to IUPAC classification, with a hysteresis loop suggesting a mixed microporous and

Table 1 Proximate analysis (wt%) of DF

		Dipterocarpus alatus fruit		
Parameter	Method	Endocarp	Pericarp	Wing
Moisture	ASTM D2867: 150 °C, 3 h	8.3	8.7	8.1
Volatile matter	ASTM D5832-98: 950 °C, 30 min	73.0	72.4	72.1
Fixed carbon	By difference	16.0	16.7	17.3
Ash	800 °C for 2 h (ref. 27)	2.7	2.2	2.5

mesoporous structure.[30] The presence of hysteresis loop is associated with the capillary condensation of N_2. The sample prepared from DF wings with $ZnCl_2$ presents a maximum uptake of nitrogen.

Porous characteristics of activated carbons obtained from the nitrogen gas adsorption–desorption isotherms were summarized in Table S1.† It was observed each part of DF (wing, endocarp and pericarp) and activating agent influenced the porosity of the resulting activated carbon. DF activated carbon contained both micropore and mesopore volume. According to IUPAC classification, adsorbent pores are classified into three groups: microspores (<2 nm), mesoporous (2–50 nm) and macrospores (>50 nm). As seen in the Table S1,† the average pore diameters of prepared carbons are in the range 2.05–2.90 nm. Therefore, there is a mixture of microporous and mesoporous carbon adsorbents. The maximum BET surface area was demonstrated through $ZnCl_2$ activation of DF wing, 843 $m^2\ g^{-1}$, micropore volume was 0.256 $cm^3\ g^{-1}$ corresponding to 54% of total pore volume and the mesopore volume, calculated by difference, was equal to 0.217 $cm^3\ g^{-1}$, which corresponding to 46% of total pore volume. This indicates the presence of a mixture of micropore and mesopore features within the activated carbon. The presence of mesoporous in combination with microspores is expected to play a significant role in the adsorption of large molecules of adsorbates including dye molecules.[21] Therefore, this carbon was used in removal performance of MB dye from the aqueous solution. Moreover, this activated carbon demonstrated an average pore diameter of 2.24 nm. The average pore size defines the ability of the adsorbate molecules to penetrate inside the activated carbon. Thus, for the adsorbate molecules to be able to penetrate the adsorbent, the pores must have a diameter larger than the molecular diameter of the adsorbate.[30] Since MB has molecular diameter of nearly 1.43 nm,[4,31] the average pore size presented by this activated carbon is suitable for MB adsorption.

The yield of activated carbon from a given precursor is an important measure of the feasibility of preparation. The effects of activating agent on the yields are shown in Table S1.† The activation with $ZnCl_2$, $FeCl_3$, H_3PO_4, CO_2 and steam resulted in carbon yields in the range of 30–50 wt%. On the other hand, KOH activation yield activated carbons with very low amount around 15–20 wt%.

Table 2 shows a comparison of the S_{BET} of the highest surface area DF activated carbon with other reported values of carbons from biomass waste in literatures. According to the results, DF has surface areas consistent with other biomass waste carbons,[30,32–42] thus making it a suitable candidate for use as precursor in the preparation of activated carbon. Moreover, raw material used in this study can utilise lower carbonization temperatures and short pyrolysis times when compared with the production of other activated carbons from biomass. For example, the carbonization temperature and time for 30 wt% $ZnCl_2$ activation of almond shell, walnut shell, apricot stone and hazelnut shell were 750–850 °C and 2 h,[36] respectively, while DF used 500 °C for 1 h. Carbonization of black wattle bark[30] and buriti shell[37] after $ZnCl_2$ activation used temperature of 700 °C for 1 and 1.5 h, respectively. Coffee residue,[34] *Posidonia oceanica* fibres[32] and *Catalpa bignonioides*[41] fruit used carbonization temperature of 700 °C for 1 after $ZnCl_2$ activation. As such, the carbonisation method employed in this work leads to reduction in energy usage and cost for DF activated carbon materials.

3.3 Properties of optimum activated carbon

Fig. S2† demonstrates the pore size distribution as calculated by BJH method for DF wing activated carbon with $ZnCl_2$ activation. The pore distribution is defined as the degree of heterogeneity porous within the materials and is directly related to the

Table 2 BET surface area comparison of DF activated carbon with other biomass waste based chemically activated carbon reported in literatures

Precursor	Chemical Activating agent	S_{BET} ($m^2\ g^{-1}$)
Dipterocarpus alatus fruit (this study)	$ZnCl_2$	843
Black wattle bark[30]	$ZnCl_2$	415
Posidonia oceanica fibres[32]	$ZnCl_2$	503
	KOH	763
	H_3PO_4	946
Coffee residue[33]	H_3PO_4	696
Coffee residue[34]	$ZnCl_2$	890
Corncob[35]	H_3PO_4	700
Almond shell[36]	$ZnCl_2$	736
Walnut shell[36]	$ZnCl_2$	774
Apricot stone[36]	$ZnCl_2$	783
Hazelnut shell[36]	$ZnCl_2$	793
Buriti shell[37]	$ZnCl_2$	843
Waste tea[38]	CH_3CO_2K	854
Waste tea[39]	H_3PO_4	880
Sugarcane bagasse[40]	H_3PO_4	873
Fruit of *Catalpa bignonioides*[41]	$ZnCl_2$	896
Pineapple leaf[42]	$ZnCl_2$	915

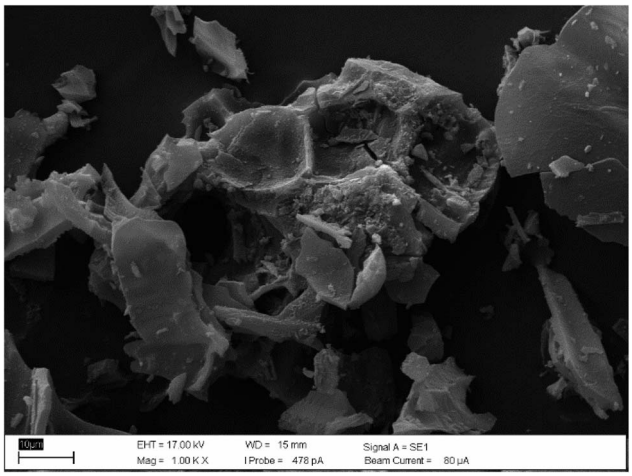

Fig. 3 SEM micrograph of $ZnCl_2$ activated carbon.

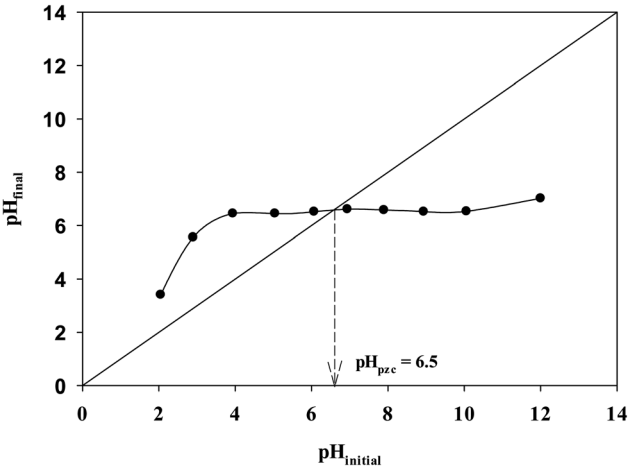

Fig. 5 Determination of point of zero charge for $ZnCl_2$ activated carbon.

adsorption equilibrium and kinetics properties of activated carbons.[37] It can be observed that the greatest proportion of pores are distributed in the region of 1.9–3.5 nm and fall into the range of micropore and mesopore, which is in agreement with the average pore diameter (2.24 nm). This means that this activated carbon include both micropores and mesopores. Therefore, DF wing activated carbon is suitable for adsorption of molecules smaller than 2.24 nm like methylene blue (1.43 nm).

The surface morphology of $ZnCl_2$ activated carbon was characterized by SEM. As shown in Fig. 3, irregular and porous surface activated carbon was observed. It can be deduced that activation with $ZnCl_2$ attacks on DF wing surface caused discontinuous surface with the formation of various sized cavities, which make up distinct micropores and mesopores. On the basis of this fact, it can be suggested that this activated carbon presents an adequate morphology for methylene blue adsorption.

Functionality of the activated carbon surface was identified with FTIR (Fig. 4). The broad band located in the region of 3100–3400 cm^{-1} related to O–H stretching vibrations existed. The band located at 1567 cm^{-1} could be attributed to C=C vibration in aromatic rings.[30] The bands at 1160 and 1093 cm^{-1} are attributed to C–O stretching in carboxyl acids, alcohols, phenols and esters.[43] The peak observed at 1093 cm^{-1} can be attributed to aromatic C–H in-plane deformation.[44] Importantly, spectra did not exhibit a significant number of absorption peaks, this attributed to black body nature of the carbonization DF.

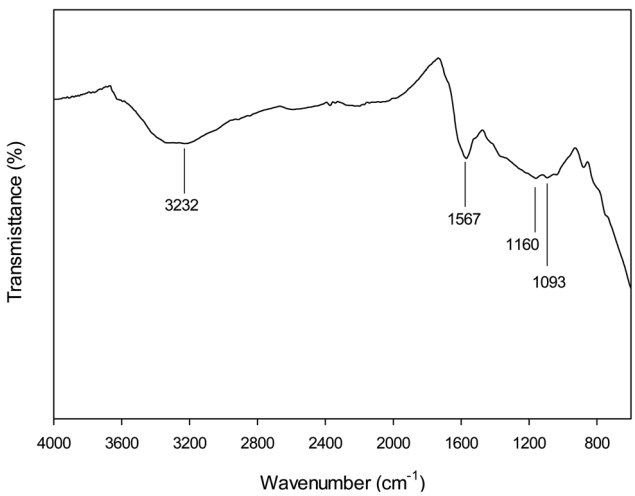

Fig. 4 FTIR spectra of $ZnCl_2$ activated carbon.

The pH_{pzc} is defined as the pH value at which the net surface charge is zero. The plot to determine the pH_{pzc} for $ZnCl_2$ activated carbon is depicted in Fig. 5. The pH_{pzc} of the optimum activated carbon is 6.5 and $pH_{pzc} < 7$ shows dominant of acidic groups over basic groups.[30] This indicating that this activated carbon is a more efficient adsorbent for the removal of cationic dyes, such as methylene blue. When solution pH < pH_{pzc}, activated carbon adsorbent will act as a positive surface, while it will act as a negative surface when solution pH > pH_{pzc}. Therefore, under low pH conditions, the electrostatic repulsion between the positively charged activated carbon surface and cationic MB dye molecules will inhibit the adsorption of MB and the presence of excess hydrogen ions may compete with MB molecules for adsorption sites. As the pH increase, the surface of activated carbon become negatively charged due to the deprotonation of the surface, which will facilitate the adsorption of MB, thus, the adsorption amount of MB increased. Foo and Hameed[45] studied the effect of pH (between pH 2–12) on MB adsorption with orange peel based activated carbon with pH_{pzc} 6.33. They found that the MB removal rose continuously with increasing pH of solution. In this current research study pH of solution was not adjusted to better mimic real applications and pH used was

Table 3 Proximate analysis (wt%) of $ZnCl_2$ activated carbon

Property	Moisture	Volatile matter	Fixed carbon	Ash
wt%	12.12	23.08	56.39	7.69

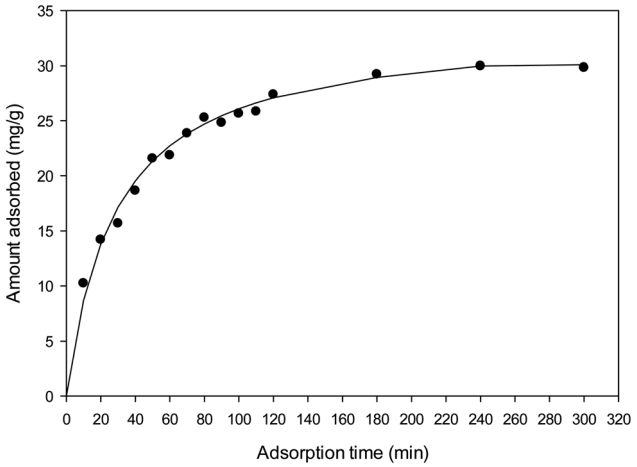

Fig. 6 The effect of contact time on the MB adsorption of $ZnCl_2$ activated carbon.

between 6.0–6.5. This is within the permitted pH of wastewater for the Thailand Standard, which must be in the range of 5.5–9.0, the neutral conditions were more suitable for MB removal by DF activated carbon in practical application. However, it is expect that the amount of MB adsorbed will increase when solution pH higher than 6.5. Moreover, the electrostatic interactions was not the only mechanism for MB removal, some other factors such as pore size of adsorbent also play important roles in MB removal.

The results for proximate analysis of the activated carbon sample are tabulated in Table 3. As expected, activated carbon has higher content of fixed carbon and lower content of volatile matter when compare with raw material, as previously demonstrated in Table 1, due to loss of volatiles during the carbonization process. The low volatile matter and ash content of activated carbon is best suited for industrial purpose.[46] High ash content can lead to a decrease in adsorptive properties and increase hydrophilicity causing restructuring process during regeneration of used activated carbon.[46] DF carbon had low ash content around 7.69 wt%, which suggests that the wing of DF used can be a good source for production of activated carbon. The similar trends of all properties have also been reported in literatures.[22,47,48]

3.4 Methylene blue adsorption

3.4.1 Effect of contact time and adsorption kinetics. Batch adsorption experiments have been achieved to detect methylene blue (MB) adsorption potential by activated carbon from DF. The effect of contact time on the removal of MB is shown in Fig. 6. The adsorption of MB on $ZnCl_2$ activated carbon was increased rapidly in first 120 min and then increased slowly until the equilibrium was reached. Adsorption equilibrium time was observed at 180 min and this time was chosen to study adsorption isotherm. For the adsorption of MB onto activated

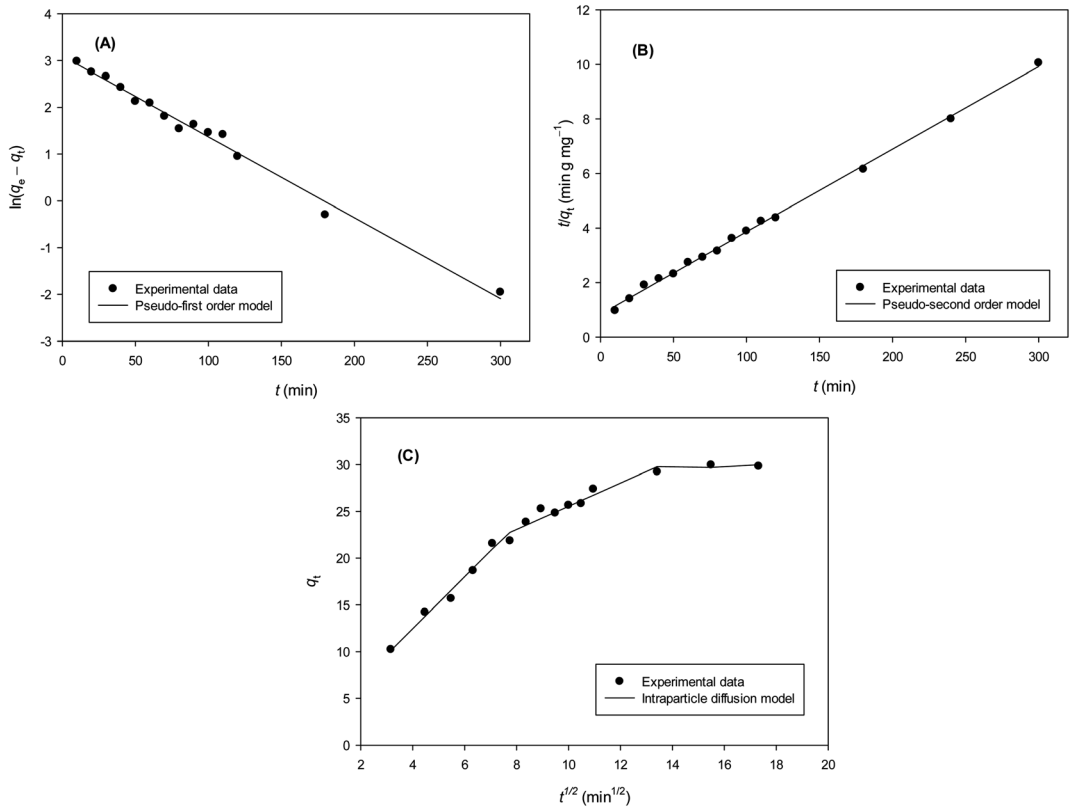

Fig. 7 (A) Pseudo-first order, (B) pseudo-second order and (C) intraparticle diffusion kinetic models for MB adsorption onto $ZnCl_2$ activated carbon.

Table 4 Parameters of pseudo-first order and pseudo-second order kinetic models

	Pseudo-first order			Pseudo-second order		
$q_{e,exp}$ (mg g^{-1})	q_e (mg g^{-1})	k_1 (min^{-1})	R^2	q_e (mg g^{-1})	k_2 (g mg^{-1} min^{-1})	R^2
29.968	22.151	0.0173	0.9897	33.003	1.099×10^{-3}	0.9983

carbons with different sources, various equilibrium times have been reported in the literature. For example, equilibrium time was found to be 250 min for activated carbon prepared from Jute fibre.[49] Hameed *et al.* reported that contact time necessary for MB dye removal using bamboo-based activated carbons reach equilibrium is 6 and 24 h.[50] Tan *et al.* also shown that using oil palm fibre activated carbons to adsorb MB were reach equilibrium within 1, 6 and 24 h.[1] Moreover, date pits activated carbon can remove MB until equilibrium within 4.5 h.[5] This indicated that activated carbon prepared from DF wing can remove MB faster than some activated carbons.

The adsorption kinetics of MB onto $ZnCl_2$ activated carbon was investigated by pseudo-first order and pseudo-second order models. The pseudo-first order kinetic model can be written in the linear form by:

$$\ln(q_e - q_t) = \ln q_e - k_1 t \quad (4)$$

where q_e and q_t are the amount of MB adsorbed on the activated carbon in mg g^{-1} at equilibrium and at any time t (min), respectively, and k_1 is the rate constant of the first-order model (min^{-1}). If the first-order kinetic model is applicable, the linear plot of $\ln(q_e - q_t)$ *versus* t must give linear plot and the value of k_1 and q_e can be determined from the slope and intercept of the plot, respectively.

The linear form of pseudo-second order kinetic model has the form:

$$\frac{t}{q_t} = \frac{1}{k_2 q_e^2} + \frac{t}{q_e} \quad (5)$$

where k_2 is the rate constant of the second-order model (g mg^{-1} min^{-1}). If the model is applicable, the plot of t/q_t against t gives a linear plot and the values of q_e and k_2 can be calculated from the slope and intercept, respectively.

The effect of intra-particle diffusion resistance on adsorption can be determined by the Weber–Morris kinetics equation:

$$q_t = k_{int} t^{1/2} + C \quad (6)$$

where k_{int} is the intraparticle diffusion rate constant (mg g^{-1} min$^{-1/2}$) and C is the constant related to the boundary layer effect of adsorption (mg g^{-1}). Fig. 7 demonstrates the results of all three kinetic models.

The rate constants and q_e values for both kinetic models are given in Table 4. The feasibility of the models is dependent on the closeness of theoretical and experimental q_e value and the highness of regression coefficients (R^2) to unity. It was shown that high R^2 values were obtained for both models but a more closeness of theoretical and experimental q_e values were achieved for pseudo-second order. This indicating that MB adsorption process onto activated carbon from wing part of DF activated with $ZnCl_2$ was better explained by pseudo-second order kinetic model. These facts suggest that the overall rate of dye adsorption process appears to be controlled by the chemisorption process involving covalent forces through sharing or exchange of electrons between surface functional groups of adsorbent and the positive charged of MB ions.[17,51,52] This model also explains the external liquid film diffusion, surface adsorption and intra-particle diffusion processes coexisted during adsorption.[53] This confirm by intraparticle diffusion model (Fig. 7). If the plots of q_t *versus* $t^{1/2}$ yields a straight line and pass through the origin, intraparticle diffusion is the controlling step. The linear plot in this study exhibit multilinearity and did not pass through the origin suggesting that intraparticle diffusion was not the only rate controlling step but some other mechanism would be involved in the adsorption process.[54] The first sharper linear portion is the instantaneous adsorption or external surface adsorption. The second linear portion is the gradual adsorption stage, where the intraparticle diffusion is the rate limiting. The third plateau linear portion is the final equilibrium stage where intraparticle diffusion starts to slow down due to extremely low adsorbate concentrations left in the solutions.[5] Many researches also confirmed that adsorption of methylene blue by using activated carbons from lignocellulosic materials follow the pseudo-second order kinetic model.[1,7,17,51,52]

3.4.2 Adsorption isotherms. Equilibrium data, which is generally known as the adsorption isotherms, is use to describe

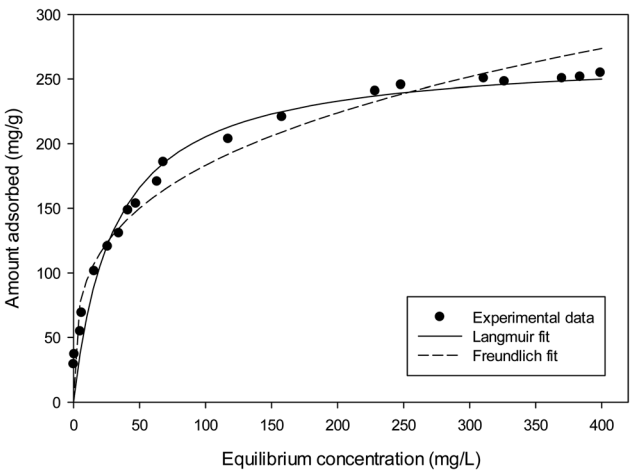

Fig. 8 Model fit of adsorption isotherm of MB adsorption onto $ZnCl_2$ activated carbon.

Table 5 Langmuir and Freundlich adsorption constants for adsorption of MB on $ZnCl_2$ activated carbon

Langmuir			Freundlich		
q_m (mg g^{-1})	K_L (L mg^{-1})	R^2	$1/n$	K_F ((mg g^{-1}) (L mg^{-1})$1/n$)	R^2
269.3	0.032	0.991	0.289	48.380	0.974

the adsorption mechanism. Adsorption isotherms describe how molecules or ions of adsorbate interact with adsorbent surface sites and optimize the use of adsorbent by predicting the maximum adsorption capacity.[20] In this study, two adsorption isotherms, Langmuir and Freundlich isotherms, were applied to experimental data for the adsorption of MB onto $ZnCl_2$ activated carbon.

The Langmuir isotherm assumes monolayer coverage of adsorbate over a homogeneous adsorbent surface and expressed as follows:

$$q_e = \frac{q_m K_L C_e}{1 + K_L C_e} \quad (7)$$

where q_e is the amount of MB adsorbed per unit mass of activated carbon under equilibrium (mg g^{-1}), q_m is the maximum adsorption capacity (mg g^{-1}), K_L represents the Langmuir constant (L mg^{-1}), and C_e stands for the equilibrium concentration of MB (mg L^{-1}). The Freundlich isotherm is based on a heterogeneous surface and used for the multilayer adsorption. The Freundlich equation is represented as follows:

$$q_e = K_F C_e^{1/n} \quad (8)$$

where K_F and n are Freundlich constants.

The Langmuir and Freundlich adsorption isotherms are shown in Fig. 8 and the isotherm constants values were given in Table 5. It can be seen that Langmuir isotherm model fitted the experimental data better than that of the Freundlich isotherm with a high correlation coefficient ($R^2 = 0.991$). It has been observed that the maximum adsorption capacity (q_m) was found to be 269.3 mg g^{-1}. The $1/n$ value from Freundlich model is 0.289 or $n = 3.46$, which n is greater than 1, indicating that the adsorption of MB on this activated carbon is favourable.[35,39] Several reports have corroborated that MB adsorption by activated carbons from lignocellulosic materials demonstrate a strong correlation with the Langmuir isotherm equation.[1,7,17,29,51]

Table 6 Comparison between DF activated carbon and other activated carbons prepared from biomass waste used for methylene blue adsorption

Precursor	q_{max} (mg g^{-1})
Dipterocarpus alatus fruit (wing)	269.3
Rice husk[55]	33.9
Ficus carica bast[51]	47.6
Coconut leaves[6]	66.0
Cashew nut shell[56]	68.7
Black wattle bark[30]	98.6
Euphorbia rigida wood[57]	114.4
Safflower seed press cake[21]	128.2
Paspalum scrobiculatum (millet husk)[58]	166.3
Coffee ground[59]	181.8
Vigna mungo L (black gram husk)[58]	198.8
Hazelnut husk[7]	204.0
Cocoa shell[52]	212.8
Citrullus lanatus rind (watermelon rind)[8]	259.7
Coffee husk[60]	263.0
Buriti shell[37]	274.6
Oil palm fibre[1]	277.8
Rattan sawdust[17]	294.1
Fruit of *Catalpa bignonioides*[41]	299.4

The maximum adsorption capacity of MB onto DF activated carbon along with that of other activated carbons, prepared from diverse biomass precursors are summarized in Table 6. Literature data was used as a basis for comparison of adsorption capacities (although they were obtained under different experimental conditions). The results in this table showed that the DF activated carbon can be effectively used for the removal of cationic dye from aqueous solution, in which its adsorption capacity is higher than many activated carbons derived from biomass waste.

The regeneration ability is also an important factor for an excellent adsorbent. After spent the activated carbon as MB adsorbents, Pathania *et al.*[51] used 1% of HCl, H_2SO_4 and NaOH to studied desorption and investigated recycling efficiency. They found that NaOH was to be an efficient desorption medium and adsorption efficiency reduced to 45% from 90% after six cycles. Future work will focus on developing methods for regeneration and reuse of the adsorbents in this study.

4 Conclusions

In this work, activated carbons were prepared from three parts of *Dipterocarpus alatus* fruit: wing, endocarp and pericarp by chemical and physical activation for methylene blue adsorption. The properties of the activated carbons are strongly dependent on the type of activating agents. The optimal activated carbon produced from wing part by chemical activation with $ZnCl_2$ attained maximum value of BET surface area as 843 m^2 g^{-1}. The equilibrium data of methylene blue adsorption onto optimal activated carbon followed the Langmuir isotherm model, showing the maximum monolayer adsorption capacity of 269.3 mg g^{-1}. The rate of adsorption was determined to follow pseudo-second order kinetic model and the parameters calculated from this model are close to experimental data. The adsorption of *Dipterocarpus alatus* fruit activated carbon of methylene blue was better than many other activated carbons made from biomass wastes in the view of adsorption capacity

and rate of adsorption. Consequently, *Dipterocarpus alatus* fruit activated carbon can be used as a low cost adsorbent for solving many environmental pollution problems and other applications.

Conflicts of interest

There are no conflicts of interest to declare.

Acknowledgements

This study was funded by Research and Academic Services Affairs of Khon Kaen University under Yang Na Scholarship.

References

1 I. A. W. Tan, B. H. Hameed and A. L. Ahmad, *Chem. Eng. J.*, 2007, **127**, 111.
2 R. Kant, *Nat. Sci.*, 2012, **4**, 22.
3 H. Du, J. Cheng, M. Wang, M. Tian, X. Yang and Q. Wang, *Diam. Relat. Mater.*, 2020, **102**, 107646.
4 A. M. M. Vargas, A. L. Cazetta, M. H. Kunita, T. L. Silva and V. C. Almeida, *Chem. Eng. J.*, 2011, **168**, 722.
5 S. K. Theydan and M. J. Ahmed, *J. Anal. Appl. Pyrolysis*, 2012, **97**, 116.
6 R. A. Rashid, A. H. Jawad, M. A. B. M. Ishak and N. N. Kasim, *Sains Malays.*, 2018, **47**, 603.
7 C. Ozer, M. Imamoglu, Y. Turhan and F. Boysan, *Toxicol. Environ. Chem.*, 2012, **94**, 1283.
8 Y. Lina, S. Wua, X. Li, X. Wu, C. Yang, G. Zenga, Y. Penga, Q. Zhoua and L. Lub, *Appl. Catal., B*, 2018, **227**, 557.
9 X. Inthapanya, S. Wu, Z. Han, G. Zeng, M. Wu and C. Yang, *Environ. Sci. Pollut. Res. Int.*, 2019, **26**, 5944.
10 O. Üner, Ü. Geçgel and Y. Bayrak, *Water, Air, Soil Pollut.*, 2016, **227**, 247.
11 G. Ma, D. Guo, K. Sun, H. Peng, Q. Yang, X. Zhou, X. Zhao and Z. Lei, *RSC Adv.*, 2015, **5**, 64704.
12 Z. Peng, Z. Guo, W. Chu and M. Wei, *RSC Adv.*, 2016, **6**, 42019.
13 E. Saputra, S. Muhammad, H. Sun and S. Wang, *RSC Adv.*, 2013, **3**, 21905.
14 M. Rasapoor, B. Young, A. Asadov, R. Brar, A. K. Sarmah, W.-Q. Zhuang and S. Baroutian, *Energy Convers. Manage.*, 2020, **203**, 112221.
15 Y. Nishimura, M. Suda, M. Kuroha, H. Kobayashi, K. Nakajima and A. Fukuoka, *Carbohydr. Res.*, 2019, **486**, 107826.
16 E. S. Seyrek, E. Yalçin, M. Yilmaz, B. V. Kök and H. Arslanoglu, *Constr. Build. Mater.*, 2020, **240**, 117921.
17 B. H. Hameed, A. L. Ahmad and K. N. A. Latiff, *Dyes Pigments*, 2007, **75**, 143.
18 C. Suiuay, S. Sudajan, S. Katekaew, K. Senawong and K. Laloon, *Energy*, 2019, **187**, 115967.
19 J. Pallarés, A. González-Cencerrado and I. Arauzo, *Biomass Bioenergy*, 2018, **115**, 64.
20 H. Demiral and C. Güngör, *J. Clean. Prod.*, 2016, **124**, 103.
21 D. Angın, E. Altintig and T. E. Köse, *Bioresour. Technol.*, 2013, **148**, 542.
22 S. Yorgun and D. Yildiz, *J. Taiwan Inst. Chem. Eng.*, 2015, **53**, 122.
23 J. F. González, S. Román, J. M. Encinar and G. Martínez, *J. Anal. Appl. Pyrolysis*, 2009, **85**, 134.
24 H. Darmstadt, M. Garcia-Perez, A. Chaala, N. Z. Cao and C. Roy, *Carbon*, 2001, **39**, 815.
25 G. H. Oh and C. R. Park, *Fuel*, 2002, **81**, 327.
26 T. Uysal, G. Duman, Y. Onal, I. Yasa and J. Yanik, *J. Anal. Appl. Pyrolysis*, 2014, **108**, 47.
27 A. Aygün, S. Yenisoy-Karakaş and I. Duman, *Microporous Mesoporous Mater.*, 2003, **66**, 189.
28 A. Heidari and H. Younesi, *J. Taiwan Inst. Chem. Eng.*, 2014, **45**, 579.
29 K. Fu, Q. Yue, B. Gao, S. Yuanyuan and Z. Liujia, *Chem. Eng. J.*, 2013, **228**, 1074.
30 S. F. Lütke, A. V. Igansi, L. Pegoraro, G. L. Dotto, L. A. A. Pinto and T. R. S. Cadaval Jr, *J. Environ. Chem. Eng.*, 2019, **7**, 103396.
31 *Water Pollution X*, ed. A. M. Marinov and C. A. Brebbia, WIT Press, 2010, p. 345.
32 M. C. Ncibi, R. Ranguin, M. J. Pintor, V. Jeanne-Rose, M. Sillanpää and S. Gaspard, *J. Anal. Appl. Pyrolysis*, 2014, **109**, 205.
33 N. F. Tehrani, J. S. Aznar and Y. Kiros, *J. Clean. Prod.*, 2015, **91**, 64.
34 F. Boudrahem, F. Aissani-Benissad and H. Aït-Amar, *J. Environ. Manage.*, 2009, **90**, 3031.
35 G. O. El-Sayed, M. M. Yehia and A. A. Asaad, *Water Resour. Data Indiana*, 2014, **7–8**, 66.
36 A. Aygün, S. Yenisoy-Karakaş and I. Duman, *Microporous Mesoporous Mater.*, 2003, **66**, 189.
37 O. Pezoti Jr, A. L. Cazetta, I. P. A. F. Souza, K. C. Bedin, A. C. Martins, T. L. Silva and V. C. Almeida, *J. Ind. Eng. Chem.*, 2914, **20**, 4401.
38 M. Auta and B. H. Hameed, *Chem. Eng. J.*, 2011, **175**, 233.
39 Y. Kan, Q. Yue, D. Li, Y. Wu and B. Gao, *J. Taiwan Inst. Chem. Eng.*, 2017, **71**, 494.
40 Y. Guo, C. Tan, J. Sun, W. Li, J. Zhang and C. Zhao, *Chem. Eng. J.*, 2020, **381**, 122736.
41 Ü. Geçel, B. Kocabıyık and O. Üner, *Water, Air, Soil Pollut.*, 2015, 226.
42 M. N. Mahamad, M. A. A. Zaini and Z. A. Zakaria, *Int. Biodeterior. Biodegrad.*, 2015, **102**, 274.
43 H. Sayğılı and F. Güzel, *J. Clean. Prod.*, 2016, **113**, 995.
44 E. Yagmur, Y. Gokce, S. Tekin, N. I. Semerci and Z. Aktas, *Fuel*, 2020, **267**, 117232.
45 K. Y. Foo and B. H. Hameed, *Bioresour. Technol.*, 2012, **104**, 679.
46 D. Kibami, C. Pongener, K. S. Rao and D. Sinha, *Chem. Sin.*, 2014, **5**, 46.
47 A. R. Hidayua, N. F. Mohamad, S. Matali and A. S. A. K. Sharifah, *Procedia Eng.*, 2013, **68**, 379.
48 N. K. E. M. Yahaya, M. F. P. M. Latiff, I. Abustan, O. S. Bello and M. A. Ahmad, *Int. J. Comput. Sci. Eng. Technol.*, 2011, **11**, 164.

49 S. Senthilkumaar, P. R. Varadarajan, K. Porkodi and C. V. Subbhuraam, *J. Colloid Interface Sci.*, 2005, **284**, 78.
50 B. H. Hameed, A. T. M. Din and A. L. Ahmad, *J. Hazard. Mater.*, 2007, **141**, 819.
51 D. Pathania, S. Sharma and P. Singh, *Arab. J. Chem.*, 2017, **10**, S1445.
52 F. Ahmad, W. M. A. W. Daud, M. A. Ahmad and R. Radzi, *Chem. Eng. Res. Des.*, 2012, **90**, 1480.
53 S. Fan, Y. Wang, Z. Wang, J. Tang and X. Li, *J. Environ. Chem. Eng.*, 2017, **5**, 601.
54 J. Pang, F. Fu, Z. Ding, J. Lu, N. Li and B. Tang, *J. Taiwan Inst. Chem. Eng.*, 2017, **77**, 168.
55 A. Dorothy and A. S. Mideen, *J. Chem. Pharm. Res.*, 2015, **7**, 761.
56 P. S. Kumar, S. Ramalingam and K. Sathishkumar, *Korean J. Chem. Eng.*, 2011, **28**, 149.
57 Ö. Gerçel, A. Özcan, A. S. Özcan and H. F. Gerçel, *Appl. Surf. Sci.*, 2007, **253**, 4843.
58 S. Valliammai, Y. Subbareddy, K. S. Nagaraja and B. Jeyaraj, *Indian J. Chem. Technol.*, 2017, **24**, 134.
59 A. Reffas, V. Bernardet, B. David, L. Reinert, M. B. Lehocine, M. Dubois, N. Batisse and L. Duclaux, *J. Hazard. Mater.*, 2010, **175**, 779.
60 L. C. A. Oliveira, E. Pereira, I. R. Guimaraes, A. Vallone, M. Pereira, J. P. Mesquita and K. Sapag, *J. Hazard. Mater.*, 2009, **165**, 87.